Nanoscale

PAPER

View Article Online
View Journal | View Issue

Cite this: *Nanoscale*, 2015, **7**, 10690

Plasmonic polymers with strong chiroptical response for sensing molecular chirality†

Dawei Zhai,‡§[a] Peng Wang,‡[a] Rong-Yao Wang,*[a] Xiaorui Tian,[b] Yinglu Ji,[c] Wenjing Zhao,[a] Luming Wang,[a] Hong Wei,[b] Xiaochun Wu[c] and Xiangdong Zhang[a]

Received 27th March 2015,
Accepted 10th May 2015

DOI: 10.1039/c5nr01966d

www.rsc.org/nanoscale

We report on the chiroptical transfer and amplification effect observed in plasmonic polymers consisting of achiral gold nanorod monomers linked by cysteine chiral molecules in an end-to-end fashion. A new strategy for controlling the hot spots based circular dichroism (CD)-active sites in plasmonic polymers was developed to realize tailored and reproducible chiroptical activity in a controlled way. We showed that by regulating the bond angles between adjacent nanorods and the degree of polymerization in the linear plasmonic polymer, weak molecular chirality in the ultraviolet spectral region can be amplified by more than two orders of magnitude *via* the induced CD response in the visible/near infrared region. We demonstrate that this plasmonic polymer can be used to provide not only the Raman "fingerprint" information for identifying the molecular identity but also the CD signatures for (i) resolving the enantiomeric pairs of cysteine molecules at a small quantity level, and (ii) quantifying the enantiomeric purity of the chiral analytes. Chiral analyses by chiroptically responsive plasmonic polymers may find important applications in bioscience and biomedicine.

I Introduction

Detection and characterization of molecular chirality are of considerable importance in biomedical science and pharmaceutics, since the two enantiomeric forms, *e.g.* the L- and D-isomer, of a biomolecule could have dramatically different impacts on our living systems.[1] Electronic/vibrational circular dichroism (CD) spectroscopy is generally used for analyzing molecular chirality, which typically measures the small differences in the interaction of left- and right-circularly polarized light with a chiral substance. However, due to inherent weak light–molecule interactions involved in the chiroptical phenomena, chiral analyses by those conventional CD spectroscopic methods are often restricted to a high concentration of analytes.[2,3] In an attempt to develop highly sensitive chiral analysis techniques, intense theoretical and experimental studies have been devoted recently to plasmon enhanced CD activity occurring in the nanocomposites composed of metallic nanoparticles (NPs) and chiral molecules.[4–19] The advances on this topic have shown a great potential of using plasmonic NPs to boost the probe sensitivity for chiral molecules.[5,13–19]

An excellent example is from discrete gold–silver (Au–Ag) core–shell nanocubes.[14] They were demonstrated to be plasmonic amplifiers for molecular chirality, showing ~100-fold CD enhancement at plasmon frequencies for DNA molecules adsorbed on the metal surfaces and enabling a trace of 0.1 μM molecular analytes to be detectable.[14] This study undoubtedly showed that molecular optical activity can be transferred to surface plasmon region with significantly enhanced intensity. However, isolated Au or Ag NPs of other shapes, such as sphere,[14] octahedron,[14] and rod,[12] showed only moderate or even non-observable CD enhancement effect for the adsorbed chiral molecules. A common feature in the latter discrete composite systems is that the involved molecule–NP interactions could not satisfy the resonant/near-resonant conditions for promoting CD enhancement effect. This situation is encountered frequently, because most of the biomolecules show absorption in the ultraviolet (UV) spectral region (150–300 nm) but the surface plasmon resonance (SPR) of ordinary Ag/Au particles locates beyond 400/500 nm in the visible/near-infrared (Vis/NIR) region. To this end, developing plasmon enhanced CD spectroscopy suitable for chirality sensing of a broad class of biomolecules is highly desirable.

[a]*Key Laboratory of Cluster Science of Ministry of Education, School of Physics, Beijing Institute of Technology, Beijing, 100081, P R China.*
E-mail: wangry@bit.edu.cn
[b]*Beijing National Laboratory for Condensed Matter Physics, Institute of Physics, Chinese Academy of Sciences, Box 603-146, Beijing, 100190, P R China*
[c]*CAS Key Laboratory of Standardization and Measurement for Nanotechnology, National Center for Nanoscience and Technology, Beijing, 100190, P R. China*

†Electronic supplementary information (ESI) available: More information for sample preparation; characterization by electron microscopy, Raman/circular dichroism (CD)/extinction spectroscopy; calculations. See DOI: 10.1039/c5nr01966d

‡Dawei Zhai and Peng Wang contributed equally to this work in performing experiments and writing the main manuscript text.

§Present address: Department of Physics and Astronomy, Ohio University, Athens, Ohio 45701, USA.

Molecularly mimetic approaches for creating plasmonic oligomers/polymers[20,21] from individual metallic NPs provide a promising solution. By virtue of a rich variety of collective optical properties arising from strong interparticle plasmon–plasmon interactions,[15–17,22–28] plasmonic oligomers/polymers were expected to possess advantages over the discrete NPs in biomolecule sensing. Indeed, benefited by strong collective chiroptical activities, chiral plasmonic dimers and oligomers produced *via* self-assembly of Au NPs have been demonstrated to be highly sensitive probes for some biomolecules like DNA and amino acids.[15–19] Even achiral plasmonic oligomers, *e.g.* linear arrangement of strongly coupled Au NPs, also showed pronounced plasmonic CD responses for ultrasensitive detection of chiral molecules.[11,19] In the case of achiral plasmonic oligomers, chiral molecules situate at the hot spots, and upon both molecular dipolar fields and external fields being greatly enhanced, molecule–NP Coulomb interactions would lead to optical transfer and amplification of molecular CD activity, from the electronic transition of the molecule in the UV region to the SPR absorption of the plasmonic nanostructure in the Vis/NIR region.[8,9,19] As such, the chiral probe by plasmon enhanced CD spectroscopy can be extended to the general molecule–NP systems with the exciton–plasmon interactions working at far off-resonant regimes.

Similar to the case of surface enhanced Raman scattering (SERS), the hot spots based CD-active sites are the core issue in achieving observable molecular chirality transfer and amplification phenomenon in the molecule–NP nanocomposites. Depending on the size of plasmonic nanogap,[8–10,15] the location and orientation of chiral molecules,[11,13,18] and the spatial arrangement of individual CD-active sites,[9,19] plasmon induced CD response can show different spectral intensities and line shapes. Thus, controlling the hot spots based CD-active sites is crucial to obtain a good reproducibility of plasmon induced CD spectral response and its amplification effect for molecular chirality. In this study, we provide a strategy for controlling the hot spots based CD-active sites in plasmonic polymers to realize tailored and reproducible chiroptical activity in a controlled way. Particularly, through manipulating the hot spot generations in gold nanorods (GNRs) polymeric structures (including the bond angles and degree of polymerization), we achieved a huge chiroptical amplification effect for molecular CD.

In our previous work,[19] we have reported a facile method for controlling molecularly mediated assembly of Au NPs into plasmonic oligomers with a good linear geometry, so as to achieve strong chiroptical transfer and amplification effect for molecular sensing. Here, this method is employed to fabricate linear chains of GNRs, *i.e.*, the plasmonic polymers, by taking advantages of the anisotropic characters of GNRs in shape and surface chemistry for facilitating unidirectional end-to-end assemblies.[29,30] For such linear plasmonic polymers, previous studies focused mainly on their nonchiral optical properties, such as localized surface plasmon resonance absorption,[31,32] surface enhanced Raman scattering,[33] and the sub-/superradiant plasmon responses.[34] By contrast, our study here is to address their chiroptically responsive properties. Specifically, we show that linear GNR polymers can present a strong and tunable plasmonic CD effect, in response to the chirality of the adsorbed cysteine (Cys) molecules at the hot spots. Controlling the bond angles and degree of polymerization in the GNR polymers allows us to realize an over two orders of magnitude of CD amplification for molecular chirality. Furthermore, this chiroptically responsive plasmonic polymer provides a powerful chiral analysis method for both resolving opposite enantiomers of a chiral molecule and quantifying the enantiomeric purity of the analytes.

II Materials and methods

Synthesis

GNRs capped with positively charged stabilizers, *i.e.* cetyltrimethylammonium bromide (CTAB), were prepared by a seed-mediated method (see the ESI†). The used GNRs, whose average length is 40.6 nm and average diameter is 17.1 nm, have a concentration of ~0.9 nM in solution. As in previous studies,[33] the linear assembly of GNRs was triggered by adding Cys (≥99%, Sigma-Aldrich), a thiol-containing amino acid with amine and carboxylic groups, into the colloidal solution of GNRs. Since the added Cys molecules would adsorb onto GNR end-surfaces by forming strong Au–S bonds, the linear self-assembly of GNRs occurred *via* Cys–Cys zwitterionic electrostatic attraction between carboxylic and amine groups.[35] Note that a repulsive force also existed between adjacent GNRs due to positively charged CTAB on the side-surfaces. As such, the balance between the attractive and repulsive forces would be a key factor to determine the bond angle between adjacent GNRs in the linear polymers. A qualitative control of bond angle was achieved in this study by simply tuning the concentration of CTAB in the as-prepared colloidal solution. Different ionic (CTA^+) strengths due to different CTAB concentrations were measured by zeta potential (ζ),[36] which is 54–57 mV for the preparation of collinear GNR polymers and 45–51 mV for zigzag polymers. Cys molecules with a concentration of 9.0 μM in the colloidal solution were used unless otherwise stated.

Characterization

Raman spectra were collected using a Leica microscope equipped with a confocal Raman spectroscopic system (Renishaw inVia) and a 6 mW 785 nm laser excitation source. A 50× objective (NA 0.5) was used for excitation and signal collection. The exposure time for acquiring the Raman spectra is 20 s. Extinction and CD spectra were recorded by a spectropolarimeter (Bio-Logic MOS-450). The optical path is 10 mm and the scan speed is 120 nm min^{-1} unless otherwise stated. Environmental scanning electron microscope (ESEM, FEI Quanta 200FEG, operated at 30 kV), which is often used to observe the biological specimens in a natural state, was used to observe our samples in a wet condition (usually by setting at the low vacuum mode. The aggregate structures observed in this wet condition should be approximate to those in the solution phase. In addition, microstructure analyses of the samples were con-

ducted by using a scanning electron microscope (SEM, JOEL, JSM-7500F) operated at 5 kV, and a transmission electron microscope (TEM, JEM-2010) operated at 200 kV.

III Results and discussion

Fig. 1A illustrates the simple method employed for controlling the interparticle bond angles to form collinear and zigzag polymers of GNRs. At a relatively high CTAB concentration, densely packed CTAB layers on the side surfaces of GNRs enable the two approaching GNRs to experience a large repulsive force from the side surfaces, hence a small bond angle would be energetically favoured (Fig. 1A, upper route). On the other hand, at a relatively low CTAB concentration, less dense package of CTAB layers and accordingly a smaller repulsive force between the GNRs would allow a relatively large bond angle between GNRs (Fig. 1A, lower route). In this way, we fabricated the linearly assembled collinear GNR polymers (Fig. 1B) and zigzag GNR polymers (Fig. 1C) (also see Fig. S1 and S2 in the ESI† for more electron microscopic images). A major difference in these two typical linear polymers is the distribution of the bond angle between adjacent GNRs. Statistical analysis based on ESEM images revealed that the collinear polymers and zigzag polymers were prevailed by the bond angles in the range of 0–20° and 101–120°, respectively (See Fig. 1D and S3 in the ESI†).

Considering that the interparticle plasmon–plasmon coupling is very sensitive to the relative orientation of neighboring GNRs,[37–40] the optical properties of these two types of linear

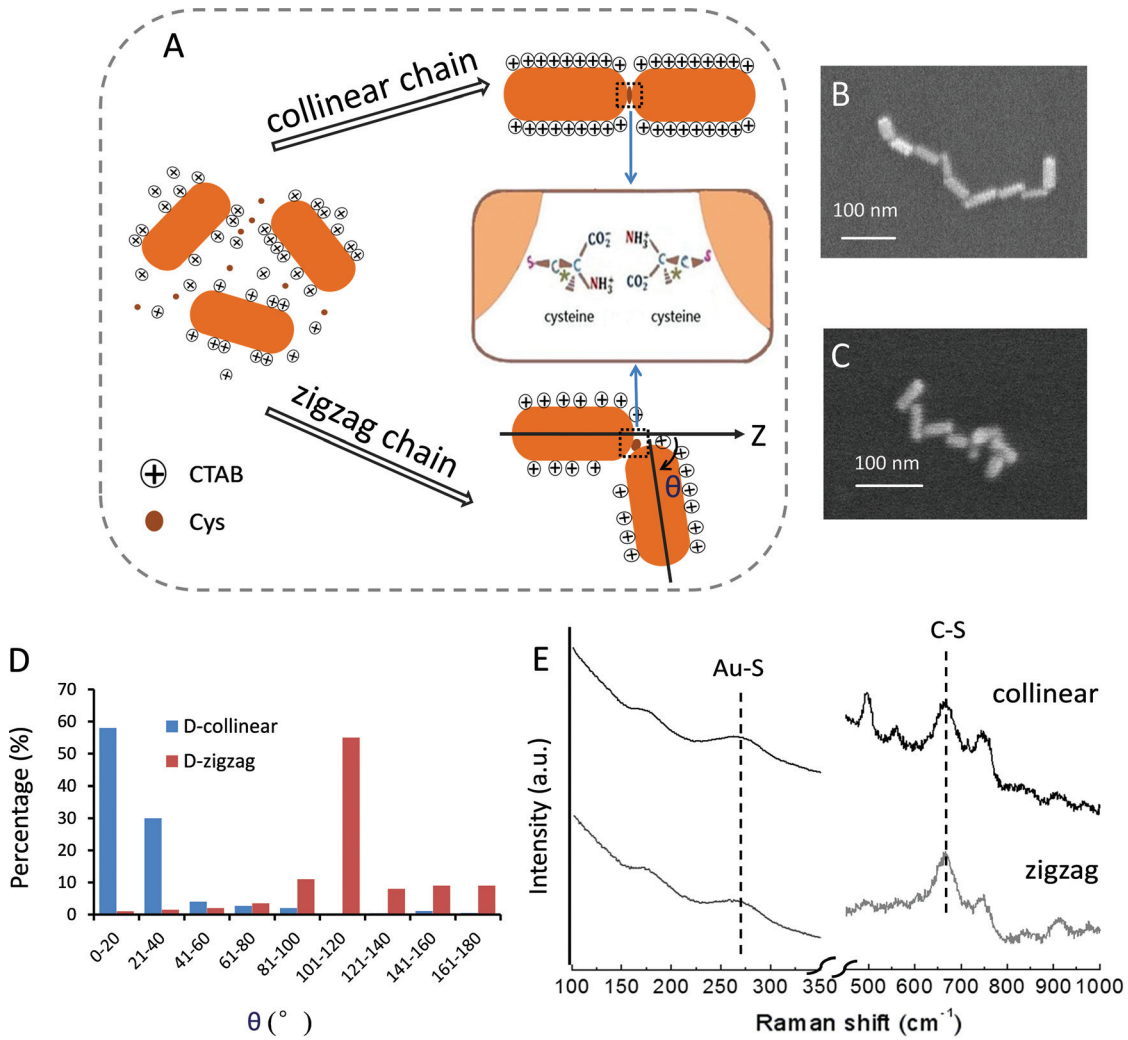

Fig. 1 (A) Schematics for Cys-mediated assembly of GNRs to form either collinear (upper route) or zigzag (lower route) polymers. The bond angle θ ($0 \leq \theta \leq 180°$) is defined by the angle between the long axes of adjacent GNRs (taking the long axis of the first GNR as the z-axis). (B, C) Representative ESEM images of collinear and zigzag polymers by using D-Cys as molecular linkers. (D) Statistical distribution of the bond angle in collinear (blue) and zigzag (brown) polymers based on the analysis from more than 500 nanorods in the ESEM micrographs. (E) SERS spectra of the collinear (upper) and zigzag (lower) GNR polymers with L-Cys linkers at the hot spots. Locations of Au–S and C–S bonds are indicated by the dashed lines. For clarity, the spectra from 450 to 1000 cm^{-1} were enlarged by 3-fold.

polymers would be different. This was verified firstly by the SERS spectra from Cys linkers located at the hot spots (Fig. 1E). The Au–S bond at ~269 cm^{-1} and the C–S stretching bond at ~665 cm^{-1} are two characteristic Raman signatures of the Cys linkers;[41,42] these Raman 'fingerprints' provide unique information for identifying Cys molecules. The peak intensities of C–S stretching mode were used to estimate the ensemble-averaged SERS enhancement factors, which are ~1.9×10^6 for the collinear polymers and ~1.0×10^6 for the zigzag polymers (see the ESI† for the details of estimations and Fig. S4†). The slightly stronger electric field enhancement in the hot spots of the collinear polymers is consistent with previous studies.[37,38]

The different electromagnetic properties of the hot spots in collinear and zigzag polymers would exert significant impact on the exciton–plasmon interactions, rendering distinguishable chiroptical properties in these two polymer structures. For the formation of zigzag polymers with L-Cys as linkers, Fig. 2A and B show the dynamic extinction and CD spectra that were recorded within the assembly time t from 0 to 10 min. The time of assembly t = 0 was referred to as the moment at which Cys molecules were added into GNR colloidal solution. The extinction spectrum (Fig. 2A, black line) of isolated GNRs displayed a longitudinal SPR band at ~640 nm and a transverse SPR band at ~515 nm. With the addition of Cys linkers, the occurrence of a linear assembly of GNRs was verified by the characteristic SPR changes with time (Fig. 2A, blue and red lines)[32,33,35]: a gradual decrease in the intensity of the longitudinal SPR mode at ~640 nm from isolated GNRs, and a concomitant growth and broadening of a new plasmon band at longer wavelengths due to strong near-field plasmon coupling between adjacent GNRs. Accompanying the SPR spectral changes, the corresponding dynamic CD signals were recorded simultaneously. As is shown in Fig. 2B, the CD intensity reached a maximum very rapidly (within 5 min of the assembly time) and then showed a plateau state afterwards. Well-resolved CD spectra within the first 5 min were not accessible by the CD instrument used, owing to a very fast kinetic process in the formation of zigzag polymers. The zigzag polymers displayed two distinct CD signatures (Fig. 2B): (1) the bisignate UV-CD in the range of 210–350 nm, which is related to the changes of molecular optical activity due to the presence of strongly coupled plasmonic NPs;[8] and (2) the bisignate plasmonic CD in the range of 500–820 nm by virtue of hot spot enhanced exciton–plasmon interaction.[8] The dynamic extinction and CD spectra acquired from the formation of zigzag polymers with D-Cys as linkers are given in the ESI (Fig. S5†). As is expected, the CD response in the case of D-Cys is inverted compared with that in the case of L-Cys.

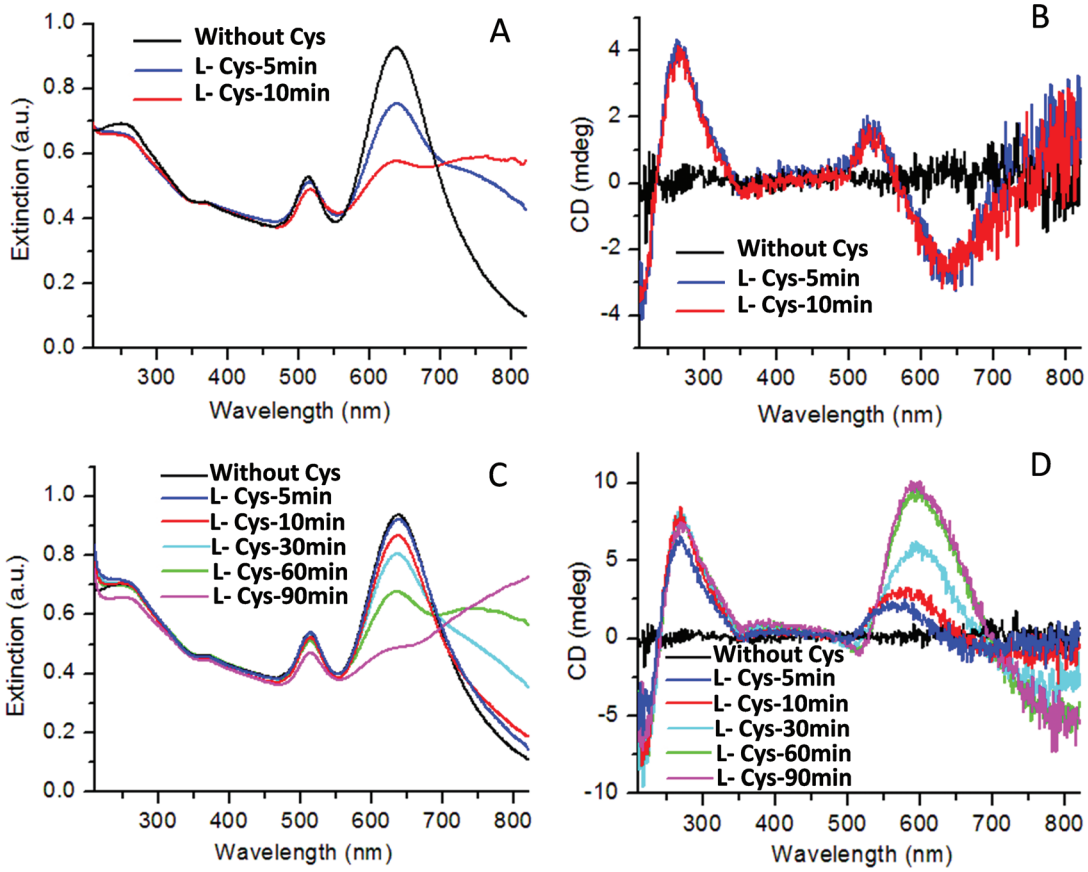

Fig. 2 Dynamic (A, C) extinction and (B, D) CD spectra acquired during the formation of zigzag (upper panel) and collinear (lower panel) GNR polymers with L-Cys (9.0 μM) as linkers. The assembly time t = 0 is referred to the moment when Cys is added into the GNR colloidal solution.

In comparison with zigzag polymers, collinear polymers showed distinct optical responses. Fig. 2C and D show the dynamic extinction and CD spectra from collinear polymers of GNRs with L-Cys as linkers, which were recorded within the assembly time t from 0 to ~90 min. The dynamic extinction spectra (Fig. 2C) also suggested the end-to-end assembly manner in the formation of GNR polymers, but exhibited much slower assembly kinetics owing to a relatively large inter-particle repulsive force experienced by the GNRs with closely packed CTAB layers on side surfaces (Fig. 1A, upper route). This slow kinetic process allowed well-resolved dynamic CD spectra to be accessible. As is shown in Fig. 2D, time-resolved plasmonic CD spectra displayed a gradual growth in intensity, a broadening in the full width at half maximum, and a red shift of the spectral peak position as well, until a saturated status was reached after t > 60 min (see the ESI Fig. S6A and S6B† for more dynamic spectra recorded in the period of t = 90–150 min). A same trend was observed in the dynamic extinction and CD spectra acquired from the formation of GNR polymers with D-Cys as linkers (ESI Fig. S6C–F†). These dynamic changes of the CD spectra within 90 min are in accordance with the spectral changes of the SPR band (Fig. 2C). According to earlier studies,[32,33] the steady red-shift of the spectral position and growth of the intensity of the SPR band were indications of the increase of degree of polymerization during the end-to-end assembly of GNRs. Likewise, correlation exists between the corresponding spectral changes (in position and strength) of the plasmonic CD signal and the degree of polymerization.

As in previous studies,[32,33] we conducted analysis of the SEM images of the collinear polymers in the course of self-assembly (within 15–90 min), in parallel with extinction/CD measurements (see the ESI† for the experimental details). The representative SEM images acquired within the assembly time of 15–90 min for collinear polymers with L- or D-Cys as linkers are given in the ESI (Fig. S7†). The aggregates in the SEM images were classified into two categories: (1) linear chains (see *e.g.* those in red circles) and (2) partially or fully disordered aggregates (see *e.g.* those in yellow circles). While a control experiment proved that the disordered aggregates would make a negligible contribution to the plasmonic CD signal (see Fig. S8†), the SPR spectroscopic information (in Fig. 2C and S6C†) acquired from the entire population of aggregates in the solution phase provided a solid support to the presence of the linear chains. As such, only the linear clusters in the SEM images (including approximately 1000 GNRs in total) were counted to estimate the degree of polymerization.

Variation of polymer length was characterized by the changes of the average aggregation number of the GNR polymers, which is defined as $\bar{X}_n = \sum n_x x / \sum n_x$, where n_x is the number of chains containing x particles.[32,33] In Fig. 3A, the derived $\bar{X}_n$ shows the linear dependence on the assembly time, which is consistent with previous results.[31] In Fig. 3B, the normalized intensities of the plasmonic CD peak at 600 nm derived from dynamic CD measurements are plotted as a function of $\bar{X}_n$. The CD strength grew dramatically with the degree of polymerization when $\bar{X}_n \lesssim 6$, then reached a plateau state and exhibited independence on further increase of assembly degree (see the results after 90 min in the ESI Fig. S6†). The collinear polymers linked by D-Cys showed similar behavior as that in the case of L-Cys but with an opposite sign in the CD signal. The dependence of CD strength on the polymer length is reminiscent of that reported in previous studies for the SERS signal from plasmonic NP chains,[33,40] which elucidated the relationship between plasmon enhanced spectroscopy and the generation of hot spots during the self-assembly of NP chains. Together with the above kinetic behavior, our results justify the hot spot-related nature of the plasmonic CD observed in the GNR polymers. They also suggest that such a molecularly induced plasmonic CD, similar to the SERS spectra reported previously,[33] can be an alternative probe of dynamic generation of hot spots during the linear assembly of GNRs.

It is noteworthy that the collinear and zigzag polymers show different CD responses, at both spectral strengths and positions. Compared with the collinear polymers, the zigzag polymers with a similar level of assembly degree exhibited a dramatic decrease in both UV-CD and plasmonic CD strength. This means that the CD-active sites at the hot spots of the zigzag polymers have poor performance in optical chirality transfer and amplification. Furthermore, since GNR dimers with smaller bond angles show the coupled plasmon modes at relatively longer wavelengths,[37,38] the CD response of the collinear polymers displayed a red-shift of the plasmonic CD peak, in comparison with that of the zigzag polymers. These results suggest that spectrally tunable chiroptical responses can be achieved by simply manipulating the bond angle and degree of polymerization in linear GNR polymers.

For the polymers of GNRs (with the aspect ratio of 2.4) formed with Cys linkers at a concentration of 9 μM, we evaluated the ensemble-averaged chiroptical amplification for Cys molecules achieved by plasmonic CD in the collinear and zigzag polymers. Note that the same amount of Cys in the absence of the GNRs showed non-detectable signal by conventional electronic CD measurement (ESI Fig. S9†). The amplification factor (AF) is defined as the ratio of plasmonic CD peak intensity to the native molecular CD peak intensity. Experimentally, AF values were estimated using $AF = (I_{PCD}/N_{surf})/(I_{ECD}/N_{vol})$, where I_{ECD} and I_{PCD} represent respectively the maximum peak intensities of CD signals from pure Cys bulk solution (at 203 nm) and from the GNR polymers (at 600/645 nm for collinear/zigzag polymers); N_{vol} is the average number of molecules in the pure Cys bulk solution in the illuminated volume; N_{surf} is the number of molecules on the end surfaces of the GNRs in the same illuminated volume. Without a precise knowledge of the number of Cys at hot spots, we estimated a low-bound AF value by assuming that all the Cys molecules that could adsorb on the end surfaces would make contributions to the observed plasmonic CD signal. Based on five independent measurements, the AF value is only ~10 ± 4 for the zigzag polymers, but is as high as 120 ± 12 for the collinear polymers (see the ESI† for the calculation details). Therefore, more than two orders of magnitude of CD enhance-

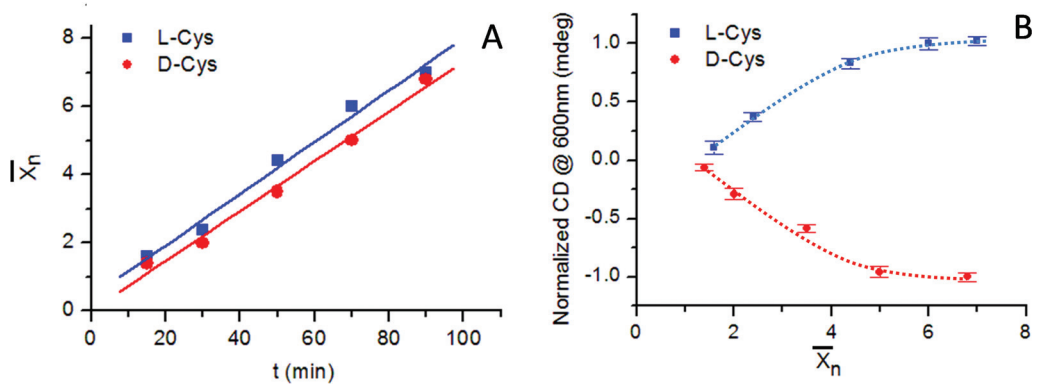

Fig. 3 (A) Variation in the average aggregation number, $\bar{X}_n$, of the collinear GNR polymers with L-Cys (blue squares) or D-Cys (red dots) as linkers, plotted *vs.* self-assembly time, *t*. Solid lines are the corresponding linear fits of the experimental data, with the Pearson coefficients of 0.993 (blue line) and 0.991 (red line). The assembly time $t = 0$ is referred to the moment when Cys is added into the GNR colloidal solution. The data points were derived from statistical analysis of ~1000 nanorods in randomly selected SEM images (representative SEM micrographs are given in Fig. S7†). (B) Normalized intensities of CD peak at 600 nm as a function of $\bar{X}_n$. Dashed lines are merely the guide lines.

ment was achieved by controlling the bond angle and the degree of polymerization in the GNR polymers. The large AF value from the collinear polymer is much higher than that reported in our previous work for Au nanosphere based plasmonic oligomers.[19] Moreover, such a giant CD amplification factor for small chiral molecules is one of the highest values reported so far from Ag and Au-based plasmonic nanostructures.

The ultrahigh CD amplification effect from the collinear polymers allows us to do chiral analysis for Cys molecules in the solution phase using the plasmonic CD spectroscopy. Fig. 4A shows the CD responses from the collinear polymers formed by adding 9 μM of enantiomer pure L-Cys (blue), D-Cys (red), or racemic mixture of D,L-Cys (black) in the GNR solutions, respectively. The corresponding extinction spectra are given in the ESI (Fig. S10†). The strong plasmonic CD responses showed a mirror-image for enantiomer pure L-Cys and D-Cys, while no CD signal was observed for the racemic mixture. For comparison, we conducted conventional electronic CD measurements for pure Cys solution in the absence of GNRs. To observe a signal with comparable magnitude as that in plasmonic CD, a much higher concentration of Cys (*e.g.* 270 μM) was required in the case of electronic CD measurement (Fig. 4A, inset). In contrast, to achieve an observable plasmonic CD signal (with an intensity larger than 1.0 mdeg), the used Cys can be as low as 0.5 μM by means of CD responsive GNR polymers (Fig. 4B, the corresponding extinction spectra are given in the ESI Fig. S11†). Such a probe is far beyond the capability of conventional electronic CD measurements. We also noticed that previous studies reported non-detectable plasmonic CD signal from the end-to-end assembled collinear chains of GNRs linked by long strands of DNA molecules.[15] This CD silence is possibly due to a weak local field enhancement at hot spots caused by a bigger size of DNA linkers, thus a larger interparticle spacing. In our case, the GNRs in the collinear polymers linked by small Cys molecules are arranged in proximity (with an average size of

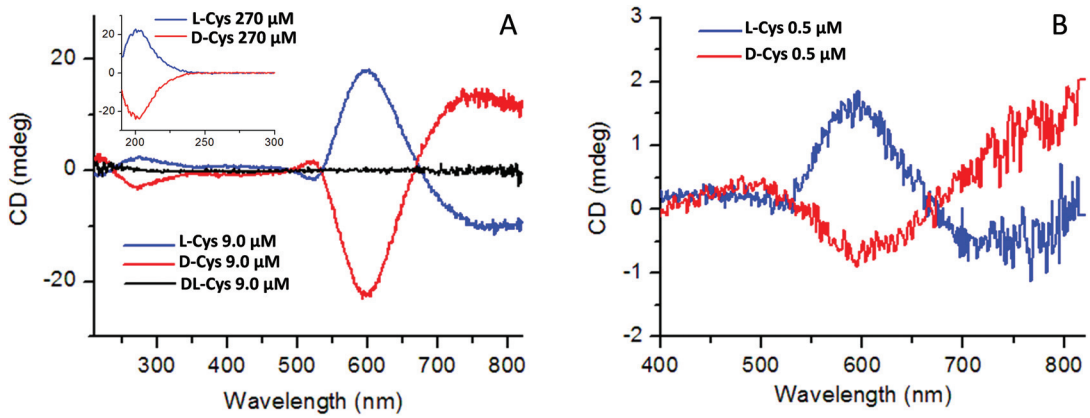

Fig. 4 (A) CD responses from collinear GNR polymers with L- (blue line), D- (red line), and D,L-Cys (black line) linkers at the hot spots. Inset: CD spectra of pure L- and D-Cys solutions (270 μM) showing the CD strength comparable with that of the plasmonic CD. (B) Mirror-image of the plasmonic CD responses of the collinear GNR polymers in the probe of L-Cys (blue line) and D-Cys (red line) molecules at the concentration of 0.5 μM.

nanogap of ~1 nm) and therefore strongly coupled to provide intense electric fields at the nanogaps. The intense local field enhanced exciton–plasmon electromagnetic interactions can facilitate a strong plasmonic CD induction effect[8] in the plasmonic polymers. These results suggest that the chiral probe by hot spot effect based CD responses of the collinear polymer is more suitable for small chiral molecules.

In previous studies,[15,16] strong plasmonic CD activity from side-by-side assembled GNR oligomers linked either through chiral or achiral molecules were used for biomolecular sensing. In this case, it is believed that molecularly induced chiral geometry (twist) with a preferred left- or right-handedness in the assembled GNR oligomers is responsible for the observed plasmonic CD effect. For such a chiral geometry-based CD effect, interparticle positions, especially the distribution of interparticle twist angles, play a crucial role in determining the sign and strength of the ensemble-averaged CD signal. Equal distribution of the opposite twist angles in the GNR oligomers would lead to a racemic mixture, hence showing inactive plasmonic CD effect.[15] Due to an inherent diversity in the interparticle relative orientations in the assembled structures, molecularly induced preference of a chiral geometry can be weakened and even eliminated due to the racemization effect that may occur particularly at a higher degree of aggregation. Indeed, earlier experimental studies have revealed that the side-by-side assembled GNR oligomers with larger sizes or higher degrees of aggregation exhibited a significant reduction of the CD signal.[15] This result implies that the chiral probe using the side-by-side twisted GNR oligomers will be severely interfered by the structural inhomogeneity that is inherent in self-assembled nanostructures.

In contrast, chiroptical responses of the collinear polymers of GNRs reported here are very robust against interference from the diversity nature of the assembled structures. As mentioned above, the chiral responsive collinear polymers showed a maximum CD signal at a certain degree of polymerization (corresponding to an assembly time t ~90 min). This maximum CD signal then exhibited an unnoticeable reduction afterwards (red and blue lines in the ESI Fig. S7B and F†), although a further growth of polymer length/size and possibly the formation of complicated structures were reflected by the dramatic changes in the corresponding extinction spectra (red and blue lines in the ESI Fig. S7A and E†).

Qualitatively, the robustness of the plasmonic CD responses against structural diversity of the GNR chain system may be taken as an indication that hot spot based CD induction, rather than chiral geometry based CD effect, makes a major contribution to the observed optical activity. However, the quantitatively distinguished contribution of the induced CD to the overall spectral signal is still a challenge. Our results shown above reveal that modification of near field distribution by regulating hot spot structures will lead to an ultrahigh amplification effect of molecular chirality. But the currently used theoretical model for plasmonic CD induction is not able to give a satisfactory explanation to such a huge chiral amplification effect. We should stress here that, due to the complexity of the composite system in solution phase, contribution of structural chirality to the plasmonic CD cannot be ruled out completely, although end-to-end assembled collinear GNR chains are expected to show negligible structural chirality.[15] More theoretical and experimental studies are still needed for a full understanding of the chiral origin in the hot spots containing composite systems composed of metallic NPs and chiral molecules.

In addition, we found that CD responses of plasmonic polymers were specific to the chirality of the probed molecules. Control experiments demonstrated that collinear GNR polymers formed *via* achiral molecules as linkers presented non-detectable plasmonic CD signals (ESI Fig. S12†). More importantly, a significant linear correlation exists between plasmonic CD signal of collinear GNR polymers and the enantiomeric excess (ee) of Cys in solution. Here ee is defined as $(M_L - M_D)/(M_L + M_D) \times 100\%$, where M_L and M_D are the fraction of L-Cys and D-Cys in the mixture ($M_L + M_D = 1$), respectively. For

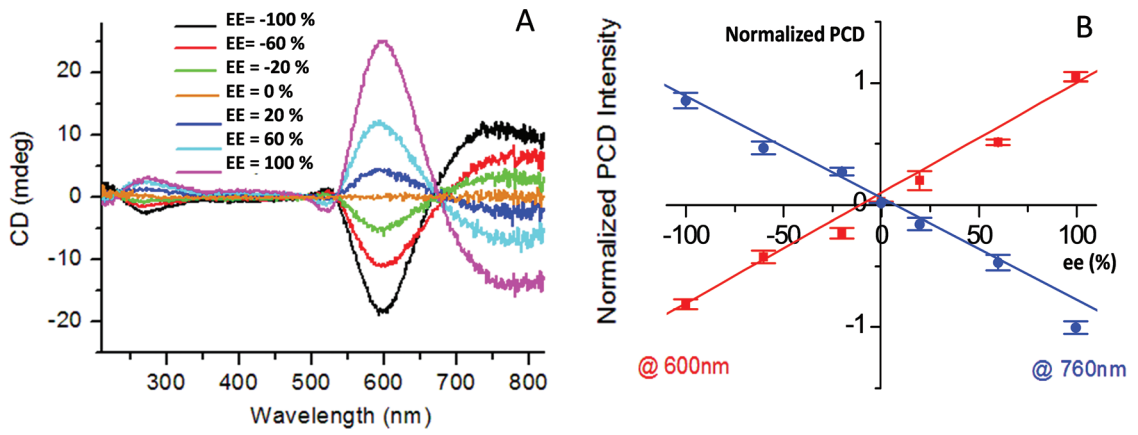

Fig. 5 (A) CD spectra of collinear GNR polymers linked by Cys molecules with different enantiomeric excess (ee). (B) Plots of the normalized CD peak/valley intensities at 600 nm (red squares) and 760 nm (blue dots) from the collinear GNR polymers as a function of the ee of Cys. The solid lines are linear fits. The Pearson coefficients are 0.992 and 0.991 for the two linear fits at 600 and 760 nm, respectively.

example, for Cys molecules with a fixed total concentration (9.0 μM), when the ee was tuned stepwise from +100% (L-Cys) to −100% (D-Cys), the sign and magnitude of the plasmonic CD signal changed accordingly (Fig. 5A, the experimental details are given in the ESI†). Fig. 5B shows the normalized peak and valley intensities of the CD bands as a function of the ee of the added Cys molecules. This demonstrates explicitly that CD responsive collinear polymers can be both an ultrasensitive chirality sensor and an ee gauge. At this point, this GNR plasmonic polymer is analogous to the chirality-responsive molecular polymer,[43,44] providing a new chirality-sensing method to determine the enantiomeric purity of the guest molecules.

IV Conclusions

We have employed a cost-effective and easy-processing method to fabricate GNRs based chiroptically responsive plasmonic polymers. The plasmonic polymers with collinear geometry can possess over two orders of magnitude of CD amplification for small chiral molecules located at the hot spots, and serve as a powerful tool for solution-based chiral analyses, including enantiomer-specific detection and enantiomeric excess quantification. In contrast to previously reported chiral plasmonic sensors, the chiral probe by our chiroptically responsive plasmonic polymers is very robust against interference by the structural diversity of the self-assembled molecule–NP composite systems. Together with their function as excellent SERS probes, plasmonic polymers with new functions for solution-based chiral detection and characterization should be novel biosensors with important applications in the fields of asymmetric chemistry, biology, and pharmaceutics.

Acknowledgements

This work was supported by the National Natural Science Foundation of China Grants (11174033, 91127013, 11134013, 11227407 and 11374012), and The Ministry of Science and Technology of China Grant (2012YQ12006005).

Notes and references

1 R. A. Sheldon, *Chirotechnology*, Dekker, New York, 1993.
2 L. D. Barron, *Molecular Light Scattering and Optical Activity*, Cambridge Univ. Press, 2004.
3 L. A. Nafie, *Vibrational Optical Activity: Principles and Applications*, Wiley, 2011.
4 I. Lieberman, G. Shemer, T. Fried, E. M. Kosower and G. Markovich, *Angew. Chem., Int. Ed.*, 2008, **47**, 4855.
5 E. Hendry, T. Carpy, J. Johnston, M. Popland, R. V. Mikhaylovskiy, A. J. Lapthorn, S. M. Kelly, L. D. Barron, N. Gadegaard and M. Kadodwala, *Nat. Nanotechnol.*, 2010, **5**, 783.
6 A. O. Govorov, Z. Fan, P. Hernandez, J. M. Slocik and R. R. Naik, *Nano Lett.*, 2010, **10**, 1374.
7 A. O. Govorov, Y. K. Gun'ko, J. M. Slocik, V. A. Gérard, Z. Fan and R. R. Naik, *J. Mater. Chem.*, 2011, **21**, 16806.
8 H. Zhang and A. O. Govorov, *Phys. Rev. B*, 2013, **87**, 075410.
9 T. Wu, J. Ren, R. Wang and X. Zhang, *J. Phys. Chem. C*, 2014, **118**, 20529.
10 B. M. Maoz, R. Weegen, Z. Fan, A. O. Govorov, G. Ellestad, N. Berova, E. W. Meijer and G. Markovich, *J. Am. Chem. Soc.*, 2012, **134**, 17807.
11 V. A. Gérard, Y. K. Gun'ko, E. Defrancq and A. O. Govorov, *Chem. Commun.*, 2011, **47**, 7383.
12 Z. Zhu, W. Liu, Z. Li, B. Han, Y. Zhou, Y. Gao and Z. Tang, *ACS Nano*, 2012, **6**, 2326.
13 B. Han, Z. Zhu, Z. Li, W. Zhang and Z. Tang, *J. Am. Chem. Soc.*, 2014, **136**, 16104.
14 F. Lu, Y. Tian, M. Liu, D. Su, H. Zhang, A. O. Govorov and O. Gang, *Nano Lett.*, 2013, **13**, 3145.
15 W. Ma, H. Kuang, L. Xu, L. Ding, C. Xu, L. Wang and N. A. Kotov, *Nat. Commun.*, 2013, **4**, 2689.
16 W. Ma, H. Kuang, L. Wang, L. Xu, W. Chang, H. Zhang, M. Sun, Y. Zhu, Y. Zhao, L. Liu, C. Xu, S. Link and N. A. Kotov, *Sci. Rep.*, 2013, **3**, 1934.
17 X. Wu, L. Liu, W. Ma, H. Yin, H. Kuang, L. Wang, C. Xu and N. A. Kotov, *J. Am. Chem. Soc.*, 2013, **135**, 18629.
18 S. Hou, T. Wen, H. Zhang, W. Liu, X. Hu, R. Wang, Z. Hu and X. Wu, *Nano Res.*, 2014, **11**, 1699.
19 R. Y. Wang, P. Wang, Y. Liu, W. Zhao, D. Zhai, X. Hong, Y. Ji, X. Wu, F. Wang, D. Zhang, W. Zhang, R. Liu and X. Zhang, *J. Phys. Chem. C*, 2014, **118**, 9690.
20 A. Guerrero-Martínez, M. Grzelczak and L. M. Liz-Marzán, *ACS Nano*, 2012, **6**, 3655.
21 A. Guerrero-Martínez, J. L. Alonso-Gómez, B. Auguié, M. M. Cid and L. M. Liz-Marzán, *Nano Today*, 2011, **6**, 381.
22 Z. Fan and A. O. Govorov, *Nano Lett.*, 2010, **10**, 2580.
23 A. Guerrero-Martínez, B. Auguié, J. L. Alonso-Gómez, Z. Džolić, S. Gómez-Graña, M. Žinić, M. M. Cid and L. M. Liz-Marzán, *Angew. Chem., Int. Ed.*, 2011, **50**, 5499–5503.
24 R. Y. Wang, H. Wang, X. Wu, Y. Ji, P. Wang, Y. Qu and T. Chung, *Soft Matter*, 2011, **7**, 8370.
25 A. Kuzyk, R. Schreiber, Z. Fan, G. Pardatscher, E. Roller, A. Högele, F. C. Simmel, A. O. Govorov and T. Liedl, *Nature*, 2012, **483**, 311.
26 M. Hentschel, M. Schäferling, T. Weiss, N. Liu and H. Giessen, *Nano Lett.*, 2012, **12**, 2542.
27 P. Wang, L. Chen, R. Y. Wang, Y. Ji, D. Zhai, X. Wu, Y. Liu, K. Chen and H. Xu, *Nanoscale*, 2013, **5**, 3889.
28 X. Shen, A. Asenjo-Garcia, Q. Liu, Q. Jiang, F. J. G. de Abajo, N. Liu and B. Ding, *Nano Lett.*, 2013, **13**, 2128.
29 H. Chen, L. Shao, Q. Li and J. Wang, *Chem. Soc. Rev.*, 2013, **42**, 2679.
30 L. Vigderman, B. P. Khanal and E. R. Zubarev, *Adv. Mater.*, 2012, **24**, 4811.

31 K. Liu, Z. Nie, N. Zhao, W. Li, M. Rubinstein and E. Kumacheva, *Science*, 2010, **329**, 197.
32 K. Liu, A. Ahmed, S. Chung, K. Sugikawa, G. Wu, Z. Nie, R. Gordon and E. Kumacheva, *ACS Nano*, 2013, **7**, 5901.
33 A. Lee, G. F. S. Andrade, A. Ahmed, M. L. Souza, N. Coombs, E. Tumarkin, K. Liu, R. Gordon, A. G. Brolo and E. Kumacheva, *J. Am. Chem. Soc.*, 2011, **133**, 7563.
34 L. S. Slaughter, B. A. Willingham, W. Chang, M. H. Chester, N. Ogden and S. Link, *Nano Lett.*, 2012, **12**, 3967.
35 P. K. Sudeep, S. T. S. Joseph and K. G. Thomas, *J. Am. Chem. Soc.*, 2005, **127**, 6516.
36 S. Lee, L. J. Anderson, C. M. Payne and J. H. Hafner, *Langmuir*, 2011, **27**, 14748.
37 A. M. Funston, C. Novo, T. J. Davis and P. Mulvaney, *Nano Lett.*, 2009, **9**, 1651.
38 L. Shao, K. C. Woo, H. Chen, Z. Jin, J. Wang and H. Lin, *ACS Nano*, 2010, **4**, 3053.
39 H. Xu, E. J. Bjerneld, M. Kall and L. Borjesson, *Phys. Rev. Lett.*, 1999, **83**, 4357.
40 Z. B. Wang, B. S. Luk'yanchuk, W. Guo, S. P. Edwardson, D. J. Whitehead, L. Li, Z. Liu and K. G. Watkins, *J. Chem. Phys.*, 2008, **128**, 094705.
41 G. D. Fleming, J. J. Finnerty, M. Campos-Vallette, F. Célis, A. E. Aliaga, C. Fredes and R. Koch, *J. Raman Spectrosc.*, 2009, **40**, 632–638.
42 E. Podstawka, Y. Ozaki and L. M. Proniewicz, *Appl. Spectrosc.*, 2005, **59**, 1516.
43 H. Nakashima, J. R. Koe, K. Torimitsu and M. Fujiki, *J. Am. Chem. Soc.*, 2011, **123**, 4847.
44 G. A. Hembury, V. V. Borovkov and Y. Inoue, *Chem. Rev.*, 2008, **108**, 1.